

A Unified Theory of Unusual Anisotropic Magnetoresistance and Unidirectional Magnetoresistance in Nanoscale Bilayers

X. R. Wang^{1,2,*}

¹*School of Science and Engineering, Chinese University of Hong Kong (Shenzhen), Shenzhen 51817, China*

²*Department of Physics, The Hong Kong University of Science and Technology, Clear Water Bay, Kowloon, Hong Kong, China*

Nanoscale bilayers containing at least one magnetic layer exhibit universal unusual anisotropic magnetoresistance (UAMR) and unidirectional magnetoresistance (UMR). They are currently understood through various mechanisms related to the interconversion of charge current and spin current, giant magnetoresistance, thermal magnonic effects, thermoelectric effects, and diverse spin-dependent scattering processes. This raises a fundamental question: do the universal behaviors observed in a wide range of systems stem from underlying general principles? We demonstrate here that both UAMR and UMR arise from electron transport influenced by the magnetization vector present in the magnetic material and the interfacial potential inherent in heterostructures. Specifically, UAMR represents current-independent resistance (resistivity) of bilayers. UMR is the resistance proportional to the current although electron transports of the bilayers are the linear response to high current densities and their induced thermal gradients. Our theory introduces a novel approach that considers the interplay between the magnetization vector, thermal gradients, and the effective internal electric field at the interface. This framework provides a unified explanation for both UMR and UAMR, effectively capturing key experimental features such as dependence on current direction, magnetization orientation, film thickness, and magnetic field strength. Furthermore, it offers a universal perspective that bridges UMR and UAMR effects, enhancing our understanding of spin-dependent transport phenomena in bilayers.

The study of magnetoresistance in nanoscale multilayers has gained significant attention due to its fundamental interest and important applications in spintronic devices. The discovery of the giant magnetoresistance (MR) and the tunneling MR [1–6] opened the field of spintronics near the end of the last century. Studies of magnetotransport in recent years have given birth to many new concepts and phenomena, such as spin Seebeck [7], spin pumping [8], spin Hall MR (SMR) [9, 10]—termed as unusual anisotropic MR (UAMR) in this study—and unidirectional MR (UMR) [11–13]. Among these, UAMR and UMR have emerged as key phenomena that reflect the intricate interplay between charge transport and magnetism.

UAMR is the resistance of bilayers at low current density and depends on the directional magnetization perpendicular to the current. For a current density $\vec{j} \parallel \hat{x}$, flowing in the plane of a ferromagnet-nonmagnet (FM/NM) bilayer, the longitudinal and transverse resistivity depends on the magnetization direction \vec{m} as: $\rho_{xx} = \rho_0 + \rho_1 m_x^2 + \rho_2 m_z^2 + \rho_3 m_z^4 + \rho_4 m_x^2 m_z^2$ and $\rho_{xy} = \rho_5 m_z + \rho_6 m_z^3 + \rho_1 m_x m_y + \rho_4 m_x m_y m_z^2$. This is in contrast to the conventional anisotropic MR (AMR), which is given by $\rho_{xx} = \rho_0 + \rho_1 m_x^2$ and $\rho_{xy} = \rho_5 m_z + \rho_1 m_x m_y$. Here, the parameters ρ_i (where $i = 0, 1, \dots, 6$) are independent of the magnetization direction.

This newly observed UAMR has stimulated the development of the SMR theory [8–10], which attributes UAMR to spin/charge current interconversion and spin current transmission/reflection at bilayer interface. SMR

theory predicts $\rho_{xx} = \rho_0 + \rho_1 m_x^2 + \rho_2 m_y^2$ which has been widely used to interpret UAMR in bilayers [14–20]. The theory is also used to understand UMR [11–13], spin-torque ferromagnetic resonance [21, 22], harmonic Hall voltage [23], magnetic field sensing [24], and magnetization or Néel-vector switching [25–29]. UAMR is a ubiquitous phenomenon observed in all kinds of nanoscale multilayers made of metals, insulators, and semiconductors with strong, weak, or negligible spin-orbit interactions, as well as in systems with topological or non-topological states. Clearly, the original SMR theory cannot apply to this wide range of multilayers. As a result, alternative spin-current-related MR models have been proposed to explain the universal nature of UAMR. These include Rashba-Edelstein MR [30, 31], spin-orbit MR [32], anomalous Hall MR [33], orbital Hall MR [34], orbital Rashba-Edelstein MR [35], Hanle MR [36]). A natural question arises: Why does the same UAMR emerge from so many different microscopic origins? Why do so many different microscopic interactions exhibit the same angular dependence? Wouldn't it be more natural to expect a unified origin for UAMR? The question becomes more urgent if one notices many inherent issues in MR-like theories [37–39] and predicted ρ_{xx} not accurately aligning with most experimental observations. Indeed, a recent two-vector theory predicts exactly the observed ρ_{xx} and ρ_{xy} of UAMR [37–39]. In this two-vector theory, the key components are magnetization of ferromagnetic (FM) layers and the effective internal interfacial electric field arising at the interface between ferromagnetic (FM) and non-magnetic (NM) materials, influencing the behavior of charges and spins. These two ingredients result in the universal behaviors of UAMR in FM/NM bilayers and FM single layers, independent of the details of

* phxwan@ust.hk

microscopic interactions among electrons, lattices, spins, and magnons.

UMR is the nonlinear MR of bilayers at high current density [above 10^{10} A/m²] [11–13, 40–53]. Different from UAMR whose resistivity does not depend on the current and follows $\rho_{xx} = \rho_0 + \rho_1 m_x^2$ when \vec{m} rotates in the xy -plane, ρ_{xx} in UMR is linear in current density and is odd in m_y . Both ρ_{xx} and ρ_{xy} are sensitive to the magnetic field, film thickness, and temperature. Under an alternating current of frequency ω , single harmonic resistivity of ρ_{xx}^ω and ρ_{xy}^ω follow the behaviour of UAMR while the second harmonic resistivity of $\rho_{xx}^{2\omega}$ and $\rho_{xy}^{2\omega}$ reverses sign with the directions of current and transverse field, and has a strong 3-fold symmetry at low magnetic field and only a 1-fold symmetry of $\rho_{xx}^{2\omega} \propto m_y$ and $\rho_{xy}^{2\omega} \propto m_x$ at high magnetic field. The same behaviour is observed in a wide range of systems, including FM/NM [11–13, 40–43], FM/semiconductor [44], FM/topological insulator bilayers [45, 46], and 2D materials [53]. Its microscopic origin is still under debate. To date, UMR is attributed to multiple origins including giant MR effect, spin Hall effect and inverse spin Hall effect, the Rashba-Edelstein effect, magnon effect, spin-flip and spin-dependent scatterings, and thermal effects. Considering coexistence of UAMR and UMR in vast different systems and two vector theory can account all behaviors of UAMR [39], it is natural to ask whether two-vector theory can also explain the universal features of UMR, and this is the main theme of this study.

In this paper, we propose a unified theoretical framework that accounts for both UAMR and UMR in nanoscale bilayers. We show that the underlying physics of universal features of UAMR and UMR are electron transport under the two vectors: magnetization and interfacial field.

To be more specific, a bilayer of one FM and a non-magnetic (NM) metallic layer is considered here although it could be various combinations of materials, including ferromagnets (FM), collinear ferrimagnets, collinear antiferromagnets and 2D magnets. Both layers are nanometer thick, allowing electrons in the metallic layer(s) to experience the magnetization ($\vec{M} = M\vec{m}$) of the FM layer, regardless of whether it is a metal or an insulator, due to quantum tunneling effects. The electric field response \vec{E} to an applied current density \vec{j} flowing along the x -direction of a bilayer in the xy -plane, as illustrated in Fig. 1, should depend on the magnetization. Additionally, an interfacial field ($\vec{n} \parallel \hat{z}$), which is perpendicular to the interface and arises from chemical potential differences between the two layers, will also influence electron motion in the bilayer. This interfacial field should decay exponentially away from the interface. Under a high current density \vec{j} (larger than 10^{10} A/m²) [11–13], a thermal gradient $\nabla T = aj^2 \hat{z}$ perpendicular to the bilayer is generated due to Joule heating, where a is a device parameter. Since the thermal gradient is already a higher-order effect of the applied current, we will limit the thermal electric contribution to the electric field in the bilayer to the level

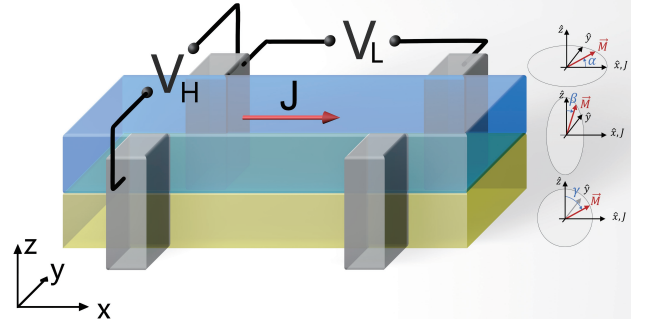


FIG. 1. Illustration of experimental set-up of a bilayer laying in the xy -plane. The blue is a FM layer and the yellow is a NM layers. Both of them are nanometer thick. They are either metal or non-metal, topological or non-topological, and can even be 2D FM and NM materials. The current flows along the x -direction. From the measurements of V_L and V_H and device geometry, one can obtain ρ_{xx} and ρ_{xy} . α is the angle between \vec{M} and the x -axis when \vec{M} rotates in the xy -plane while β and γ are the angles between \vec{M} and the z -axis when \vec{M} rotates in the yz - or xz -plane indicated in the right coordinates. Under a high current density, a thermal gradient will build up perpendicular to the bilayer (the z -direction).

of the Nernst effect. The most general expression for \vec{E} , which is linear in both \vec{j} and ∇T , is given by [54–56]

$$\vec{E} = C_0 \nabla T + C_1 \vec{m} \times \nabla T + \vec{\hat{p}}(\vec{m}, \vec{n}) \vec{j}, \quad (1)$$

where C_0 is the Seebeck coefficient and C_1 measures the anomalous Nernst effect. Thermodynamic quantities must be functions of state variables of which \vec{m} and \vec{n} are the only vectors. Thus, rank-2 resistivity tensor $\vec{\hat{p}}(\vec{m}, \vec{n})$ can only be constructed from \vec{m} and \vec{n} . Generalizing the approach from our earlier publication [37, 38] to the current case, and keeping in mind that $\nabla T \parallel \vec{n} \perp \vec{j}$, the linear response of Eq. 1 under a direct current \vec{j} leads to the longitudinal and transverse resistivity:

$$\begin{aligned} \rho_{xx} &\equiv \vec{E} \cdot \hat{x} / j = \rho + C j m_y + A_1 m_x^2 + A_2 m_z \\ \rho_{xy} &\equiv \vec{E} \cdot \hat{y} / j = -C j m_x + A_1 m_x m_y + B_1 m_z + B_2, \end{aligned} \quad (2)$$

where $C \equiv C_1 a$, ρ , A 's and B 's are device parameters and can only depend on m_z [37]. Without interfacial field, $A_2 = B_2 = 0$ and all other parameters do not depend on magnetization direction. A_1 describes usual AMR and planar Hall effect and comes from external electric field mediated electron-magnon scattering, and B_1 is the usual anomalous Hall effect. In the presence of an interfacial field, extra angular dependence of ρ_{xx} and ρ_{xy} can come from electron-magnon scattering mediated by \vec{n} , manifesting through m_z dependences of parameters. C , ρ , A_1 , and B_1 must be even functions of m_z while A_2 , A_3 , B_2 , and B_3 must be odd for achiral materials. The higher-power terms of these parameters in m_z are negligible because the power in m_z is the number of magnons involved in the scatterings. Since thermal electric effect is normally small, we shall keep C independent of m_z . If one defines $\rho = \rho_0 \sum_{n=1}^{\infty} d_n m_z^{2n}$,

$A_1 = \rho_1 + \rho_4 m_z^2 + \sum_{n=2}^{\infty} a_{1n} m_z^{2n}$; $B_1 = \sum_{n=0}^{\infty} b_{1n} m_z^{2n}$; $A_2 = \sum_{n=0}^{\infty} a_{2n} m_z^{2n+1}$; $B_2 = \sum_{n=0}^{\infty} b_{2n} m_z^{2n+1}$; $B_3 = \sum_{n=0}^{\infty} b_{3n} m_z^{2n+1}$; and keep the expansions up to \tilde{m}^4 , then the longitudinal and transverse resistivities take following universal forms

$$\begin{aligned} \rho_{xx} &= \rho_0 + \rho_1 m_x^2 + \rho_2 m_z^2 + \rho_3 m_z^4 + \rho_4 m_x^2 m_z^2 + C j m_y \\ \rho_{xy} &= \rho_5 m_z + \rho_6 m_z^3 + \rho_1 m_x m_y + \rho_4 m_x m_y m_z^2 - C j m_x, \end{aligned} \quad (3)$$

where angular-independent parameters $\rho_2 \equiv (d_1 + a_{21})$, $\rho_3 \equiv (d_2 + a_{22})$, $\rho_5 \equiv (b_{10} + b_{20})$, and $\rho_6 \equiv (b_{11} + b_{21})$. ρ_i ($i = 2, 3, 4, 6$) are from \vec{n} -mediated magnon process. Without C terms, this is exactly the behavior of UAMR observed in all kinds of multilayers including bilayers and magnetic nanoscale single layers. Interestingly, although Eq. 1 is the linear response to external forces, the resistivity appears to be nonlinear and propotional to the current density. The C -term explains well different resistances of Pt/Py bilayer when m_y [41] or j [43] is reversed at high current density ($> 10^{11} \sim 10^{12} \text{ A/m}^2$).

To separate UMR from UAMR, recent experiments [11–13, 47–53] utilize alternating current (AC) $\vec{j} = j \cos(\omega t) \hat{x}$ of frequency ω to probe magnetoresistance. By employing either frequency-locking techniques [11] or the Wheatstone bridge method [49], the first and second harmonic longitudinal and Hall voltages, denoted as V_L^ω , $V_L^{2\omega}$, V_H^ω , and $V_H^{2\omega}$ (see Fig. 1) can be measured. From them, resistances, $R_{xx}^\omega \equiv V_L^\omega/j$, $R_{xx}^{2\omega} \equiv V_L^{2\omega}/j$, $R_{xy}^\omega \equiv V_H^\omega/j$, and $R_{xy}^{2\omega} \equiv V_H^{2\omega}/j$ are obtained. When the magnetization vector \vec{m} rotates in the xy -plane at an angle α with respect to \hat{x} , universal behaviors of $R_{xx}^{2\omega} = r_1 j (\sin \alpha - \sin 3\alpha) + r_2 j \sin \alpha$ and $R_{xy}^{2\omega} = r_3 j (\cos \alpha - \cos 3\alpha) + r_4 j \cos \alpha$ are exactly what were observed across all experiments to date, while R_{xx}^ω and R_{xy}^ω exhibit UAMR behavior. We aim to demonstrate that Eq. 1 can not only explain the universal second harmonic resistivity, in addition to the UAMR for the first harmonic resistivity, but also predicts field-independent r_2 and r_4 , and negligible small r_1 and r_3 for strong magnetic field and thick bilayers.

At a high alternating current density $\vec{j} = j \cos(\omega t) \hat{x}$, an oscillating Oersted field along the y -direction $\vec{h} = dj \cos(\omega t) \hat{y}$ is generated in addition to a larger static field H that is used to control the magnetization direction \vec{m} , where d is the thickness of the bilayer. Since ω is typically less than tens of Hz in most experiments, which is significantly lower than the GHz frequency of spin response, \vec{m} should always align with the total effective field and oscillates around its averaged direction with frequency ω .

The polar and azimuthal angles of \vec{m} are $\theta + bj \cos(\omega t) \cos \theta \sin \phi$ and $\phi + bj \cos(\omega t) \cos \phi$, where θ and ϕ represent the time-averaged values, and b relates to bilayer thickness and the dynamic susceptibility of the FM layer, which is inversely proportional to the effective magnetic field [57, 58]. Thus, we can approximate $m_x(t)$, $m_y(t)$, and $m_z(t)$ as follows: $m_x(t) = \sin[\theta + bj \cos(\omega t) \cos \theta \sin \phi] \cos[\phi + bj \cos(\omega t) \cos \phi] \simeq m_x [1 - bj \cos(\omega t) \sin \phi] + bj \cos(\omega t) \cos^2 \theta \sin \phi \cos \phi$, $m_y(t) =$

$\sin[\theta + bj \cos(\omega t) \cos \theta \sin \phi] \sin[\phi + bj \cos(\omega t) \cos \phi] \simeq m_y + bj \cos(\omega t) \sin \theta \cos^2 \phi + bj \cos(\omega t) \cos^2 \theta \sin^2 \phi$, and $m_z(t) = \cos[\theta + bj \cos(\omega t) \cos \theta \sin \phi] \simeq m_z - bj \cos(\omega t) \sin \theta \cos \theta \sin \phi$. To simplify notation, we denote m_x , m_y , and m_z as the time-averaged values of $m_x(t)$, $m_y(t)$, and $m_z(t)$, respectively.

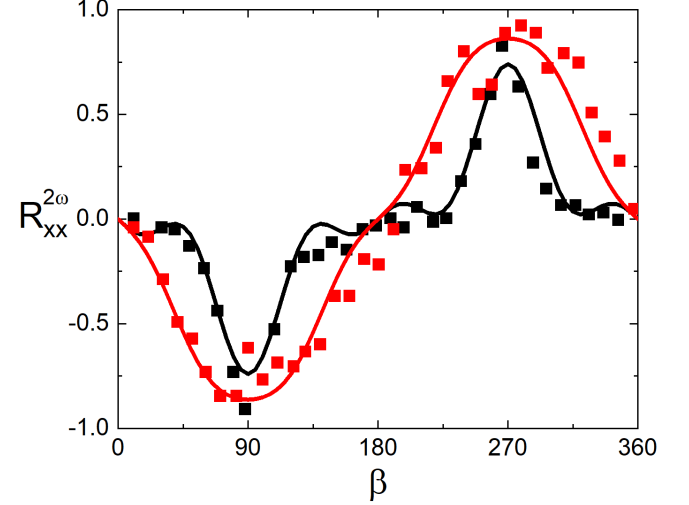


FIG. 2. Experimental data of $R_{xx}^{2\omega}(\beta)$ (symbols) and fits to $R_{xx}^{2\omega}(\beta) = a_1 \sin \beta - a_2 (\sin 3\beta - \sin \beta) - a_3 (\sin 5\beta - \sin 3\beta)$. Experimental data are from Fig. 2b of Ref. [42] for Pt(4 nm)/Co(2 nm) (the red dots) and Pt(4 nm)/Co(1 nm) (the black dots) with $j = 10^{11} \text{ A/m}^2$, $B = 2 \text{ T}$, and $\omega = 801 \text{ Hz}$. The fitting parameters are $a_1 = -0.75(-0.31) \text{ m}\Omega$, $a_2 j = -0.057(-0.086) \text{ m}\Omega$, $a_3 j = -0.041(0.14) \text{ m}\Omega$ for Pt(4 nm)/Co(2 nm) (Pt(4 nm)/Co(1 nm)).

From Eq. 1 and $\vec{\rho}(\vec{m}, \vec{n})$ established earlier [38], it follows straightforwardly that $\rho_{xx}^\omega \equiv E_x^\omega/j$ and $\rho_{xy}^\omega \equiv E_y^\omega/j$ are consistent with Eq. 3. Below, we examine how $\rho_{xx}^{2\omega} \equiv E_x^{2\omega}/j$ and $\rho_{xy}^{2\omega} \equiv E_y^{2\omega}/j$ depend on angle α when \vec{m} rotates in the xy -plane, as well as on angles β and γ when \vec{m} rotates in the yz - and zx -planes, respectively. After some algebra, we obtain:

$$\begin{aligned} \rho_{xx}^{2\omega}(\alpha) &= (C + c_1) j \sin \alpha - c_1 j \sin 3\alpha, \\ \rho_{xy}^{2\omega}(\alpha) &= -(C + c_1) j \cos \alpha + c_1 j \cos 3\alpha, \\ \rho_{xx}^{2\omega}(\beta) &= (C + c_2) j \sin \beta + (c_3 - c_2) j \sin 3\beta - c_3 j \sin 5\beta \\ \rho_{xy}^{2\omega}(\beta) &= c_4 j \sin 2\beta + c_5 j \sin 4\beta, \\ \rho_{xx}^{2\omega}(\gamma) &= 0, \\ \rho_{xy}^{2\omega}(\gamma) &= c_1 + c_6 - C j \sin \gamma - c_1 \cos 2\gamma - c_6 \cos 4\gamma, \end{aligned} \quad (4)$$

where $c_1 = \rho_1 b/2$, $c_2 = b(\rho_2 + \rho_3)/2$, $c_3 = b\rho_3/4$, $c_4 = -b(\rho_5/2 + 3\rho_6/4)$, $c_5 = -3b\rho_6/8$ and $c_6 = b\rho_4/8$. ρ_i ($i = 2, \dots, 6$) and, in turn, c_i ($i = 2, \dots, 6$) come from \vec{n} -mediated electron-magnon scattering and should decay exponentially with the layer thickness. In other words, the UAMR and UMR are mainly interfacial phenomena, and ρ_i 's and c_i 's are negligibly small for thick enough bilayers. Also c_i ($i = 1, \dots, 6$) are proportional to the dy-

dynamic susceptibility of FM layer which is inversely proportional to the effective magnetic field. Thus, all c_i -terms are negligibly small in strong magnetic field. However, C -terms in Eqs. 3 and 4 are due to the Joule heating of high current density that does not depend on the bilayer thickness and magnetic field. Although formula for $\rho_{xx}^{2\omega}(\alpha)$ and $\rho_{xy}^{2\omega}(\alpha)$ have been obtained from SMR theory and magnonic effects [11–13, 51], all existing theories have no prediction about $\rho_{xx}^{2\omega}$ and $\rho_{xy}^{2\omega}$ when \vec{m} rotates in the yz - and zx -plane, and very few measurements have been reported about longitudinal and transverse resistance (resistivity) as a function of magnetization direction in the yz - and zx -planes. To test this theory against all other existing theories, we read $R_{xx}^{2\omega}(\beta)$ [proportional to $\rho_{xx}^{2\omega}(\beta)$] from Fig. 1b in Ref. [42] and fit them by the formula in Eq. 4. The red and black dots in Fig. 2 are the experimental data for Pt(4 nm)/Co(2 nm) (red) and Pt(4 nm)/Co(1 nm) (black) with $j = 10^{11}$ A/m², $B = 2$ T, and $\omega = 801$ Hz. The curves are the fit to $R_{xx}^{2\omega}(\beta) = a_1 \sin \beta - a_2(\sin 3\beta - \sin \beta) - a_3(\sin 5\beta - \sin 3\beta)$ with fitting parameters of $a_1 = -0.75(-0.31)$ m Ω , $a_2 j = -0.057(-0.086)$ m Ω , $a_3 j = -0.041(0.14)$ m Ω for Pt(4 nm)/Co(2 nm) (Pt(4 nm)/Co(1 nm)). It is clear that the experimental data supports the current theory.

The current theory predicts that the amplitudes of 1-fold and 3-fold symmetries in $\rho_{xx}^{2\omega}(\alpha)$ are the same as the corresponding amplitudes in $\rho_{xy}^{2\omega}(\alpha)$. This prediction is consistent with all existing experiments [11–13, 47–53]. The UMR behaves differently when \vec{m} rotates in the yz -plane: $\rho_{xx}^{2\omega}(\beta)$ is the linear combination of 1-fold, 3-fold, and 5-fold sinusoidal functions while $\rho_{xy}^{2\omega}(\beta)$ is the sum of 2-fold and 4-fold sinusoidal functions. When \vec{m} rotates in the zx -plane, $\rho_{xx}^{2\omega}(\gamma)$ is zero and $\rho_{xy}^{2\omega}(\gamma)$ has a nonzero mean, 1-fold sinusoidal term, together with a 2-fold and a 4-fold cosine terms. All these predictions are new, and can be used to test and to distinguish this theory from others.

It is important to emphasize that the second harmonic signals, which are proportional to the current density, result from a linear response to the current and thermal gradient, nor a nonlinear one. The observed nonlinear behavior arises from thermal effects and current-dependent, time-dependent UAMR, as discussed above and in Eq. 1. The expressions $\rho_{xx}^{2\omega}(\alpha)$ and $\rho_{xy}^{2\omega}(\alpha)$ are exactly what were observed in all UMR experiments [11–13, 40–53]. Notably, Eq. 4 is the most general form of linear response of electron transport to a magnetization and an internal effective field perpendicular to a bilayer. In fact, if one assume magnetization is the only vector in the complete set of state variable as SMR theory assumed, then it is mathematically impossible to admit SMR formula for resistivity. The universal forms of UMR do not depend on microscopic interactions, such as sd-interaction or Rashba and Dresselhaus spin-orbit interactions. However, the thickness dependences of c_i ($i = 2, \dots, 6$) reveal the property of the interfacial field, and the external magnetic-field dependences of c_i tell us the magnetic susceptibility of the magnetic layer. It is important to

emphasize that exponential decay of UAMR in SMR-like theories is attributed to spin diffusion, not the interfacial field-mediated electron-magnon scattering. Thus, current theory predicts a stronger UAMR and UMR at a higher temperature, in agreement with experiments [52], while SMR theories would predict a weaker one, opposite to the experiments. At high fields, c_i ($i = 1, \dots, 6$) approach zero, and $\rho_{xx}^{2\omega}$ and $\rho_{xy}^{2\omega}$ become $\rho_{xx}^{2\omega}(\alpha) = Cj \sin \alpha$, $\rho_{xy}^{2\omega}(\alpha) = -Cj \cos \alpha$, $\rho_{xx}^{2\omega}(\beta) = Cj \sin \beta$, $\rho_{xy}^{2\omega}(\beta) = 0$, $\rho_{xx}^{2\omega}(\gamma) = 0$, $\rho_{xy}^{2\omega}(\gamma) = -Cj \cos \gamma$, controlled by the same coefficient C .

This work demonstrates that both UAMR and UMR can be understood within a unified theoretical framework. The interplay between magnetization, thermal gradients, and interfacial electric fields provides a comprehensive explanation for the observed phenomena. This new understanding enables the identification of materials with strong UMR effects, particularly in 2D systems and topological materials, facilitating robust UMR signals at room temperature for practical device applications. Furthermore, it allows for the integration of UMR with other spintronic effects, such as spin-orbit torque, the spin Hall effect, or magnetoelectric effects, to create multifunctional devices. For the future research, it is important to have a formulation based on microscopic Hamiltonian. Only with such a formulation one may know how to use microscopic interactions to manipulate the coefficients in UAMR and UMR.

Our findings suggest that one can select materials with the desired work function difference to control UAMR and UMR, and utilize a gate voltage to adjust the interfacial potential, which in turn can tune UAMR and UMR. UMR is considered promising for spintronic devices, especially in non-volatile memory (e.g., magnetic random-access memory, MRAM), magnetic field sensors, and spin-based logic devices. This work lays the foundation for further exploration of spin-dependent transport in multilayers and its implications for future spintronic applications. For instance, it should enhance our ability to electrically detect magnetization direction and add functionality to spintronic devices.

In conclusion, we have presented a novel theoretical approach to understanding UAMR and UMR. According to this theory, UAMR and UMR do not depend on microscopic interactions and do not require the interconversion between spin current and charge current. However, if such an interconversion can influence electron transport in a system described by only two vectors, then such a microscopic process should lead to the predictions presented here. In principle, materials with any spin-electron scattering under the influence of an interfacial potential should exhibit the universal UAMR and UMR discussed herein. Several predictions are new. Some of them are supported by existing experiments while the others are awaited for experimental confirmation.

ACKNOWLEDGMENTS

I thank Dr. Xuchong Hu for drawing the figures. This work is supported by the University Development Fund

of the Chinese University of Hong Kong, Shenzhen, the National Key Research and Development Program of China (No. 2020YFA0309600), the NSFC Grant (No. 12374122), and Hong Kong RGC Grants (No. 16300523, 16300522, and 16302321).

-
- [1] G. Binasch, P. Grunberg, F. Saurenbach, and W. Zinn, Enhanced magnetoresistance in layered magnetic structures with antiferromagnetic interlayer exchange, *Phys. Rev. B* 39, 4828(R) (1989).
 - [2] M. N. Baibich, J. M. Broto, A. Fert, F.N. Van Dau, F. Petroff, P. Etienne, G. Creuzet, A. Friederich, and J. Chazelas, Giant Magnetoresistance of (001)Fe/(001)Cr Magnetic Superlattices, *Phys. Rev. Lett.* 61, 2472(1988).
 - [3] T. Miyazaki and N. Tezuka, Giant magnetic tunneling effect in Fe/Al₂O₃/Fe junction, *J. Magn. Magn. Mater.* 139, L231(1995).
 - [4] J. S. Moodera, L. R. Kinder, T. M. Wong, and R. Meserve, Large Magnetoresistance at Room Temperature in Ferromagnetic Thin Film Tunnel Junctions, *Phys. Rev. Lett.* 74, 3273(1995).
 - [5] S. S. P. Parkin, C. Kaiser, A. Panchula, P. M. Rice, B. Hughes, M. Samant, and S-H. Yang, Giant tunnelling magnetoresistance at room temperature with MgO (100) tunnel barrier, *Nat. Mater.* 3, 862(2004).
 - [6] S. Yuasa, T. Nagahama, A. Fukushima, Y. Suzuki, and K. Ando, Giant room-temperature magnetoresistance in single-crystal Fe/MgO/Fe magnetic tunnel junctions, *Nat. Mater.* 3, 868(2004).
 - [7] K. Uchida, S. Takahashi, K. Harii, J. Ieda, W. Koshibae, K. Ando, S. Maekawa, and E. Saitoh, Observation of the spin Seebeck effect, *Nature* 455, 778(2008).
 - [8] Y. Tserkovnyak, A. Brataas, and G. E.W. Bauer, Spin pumping and magnetization dynamics in metallic multilayers, *Phys. Rev. B* 66, 224403 (2002).
 - [9] Y. T. Chen, S. Takahashi, H. Nakayama, M. Althammer, S. T. B. Goennenwein, E. Saitoh, and G. E.W. Bauer, Theory of spin Hall magnetoresistance, *Phys. Rev. B* 87, 144411 (2013).
 - [10] H. Nakayama, M. Althammer, Y.-T. Chen, K. Uchida, Y. Kajiwara, D. Kikuchi, T. Ohtani, S. Geprägs, M. Opel, S. Takahashi, R. Gross, G. E.W. Bauer, S. T. B. Goennenwein, and E. Saitoh, Spin Hall Magnetoresistance Induced by a Nonequilibrium Proximity Effect, *Phys. Rev. Lett.* 110, 206601 (2013).
 - [11] C. O. Avci, K. Garello, A. Ghosh, M. Gabureac, S. F. Alvarado, and P. Gambardella, Unidirectional spin Hall magnetoresistance in ferromagnet/normal metal bilayers, *Nat. Phys.* 11, 570 (2015).
 - [12] C. O. Avci, K. Garello, J. Mendil, A. Ghosh, N. Blasakis, M. Gabureac, M. Trassin, M. Fiebig, and P. Gambardella, Magnetoresistance of heavy and light metal/ferromagnet bilayers, *Appl. Phys. Lett.* 107, 192405 (2015).
 - [13] C. O. Avci, J. Mendil, G. S. D. Beach, and P. Gambardella, Origins of the Unidirectional Spin Hall Magnetoresistance in Metallic Bilayers, *Phys. Rev. Lett.* 121, 087207 (2018).
 - [14] T. Lin, C. Tang, H. M. Alyahyaei, and J. Shi, Experimental Investigation of the Nature of the Magnetoresistance Effects in Pd-YIG Hybrid Structures, *Phys. Rev. Lett.* 113, 037203 (2014).
 - [15] S. Cho, S.-h. C. Baek, K.-D. Lee, Y. Jo, B.-G. Park, Large spin Hall magnetoresistance and its correlation to the spin-orbit torque in W/CoFeB/MgO structures, *Sci. Rep.* 5, 14668 (2015).
 - [16] X. Zhou, L. Ma, Z. Shi, W. J. Fan, Jian-Guo Zheng, R. F. L. Evans, and S. M. Zhou, Magnetotransport in metal/insulating-ferromagnet heterostructures: Spin Hall magnetoresistance or magnetic proximity effect, *Phys. Rev. B* 92, 060402(R)(2015).
 - [17] J. Kim, P. Sheng, S. Takahashi, S. Mitani, and M. Hayashi, Spin Hall Magnetoresistance in Metallic Bilayers, *Phys. Rev. Lett.* 116, 097201 (2016).
 - [18] D. Hou, Z. Qiu, J. Barker, K. Sato, K. Yamamoto, S. Vélez, J. M. Gomez-Perez, L. E. Hueso, F. Casanova, and E. Saitoh, Tunable Sign Change of Spin Hall Magnetoresistance in Pt/NiO/YIG Structures, *Phys. Rev. Lett.* 118, 147202 (2017).
 - [19] Y. Ji, J. Miao, Y. M. Zhu, K. K. Meng, X. G. Xu, J. K. Chen, Y. Wu, Y. Jiang, Negative spin Hall magnetoresistance in antiferromagnetic Cr₂O₃/Ta bilayer at low temperature region, *Appl. Phys. Lett.* 112, 232404 (2018) .
 - [20] S.-Y. Huang, H.-Lin Li, C.-W. Chong, Y.-Y. Chang, M.-K. Lee, J.-C.-A. Huang, Interface-induced spin Hall magnetoresistance enhancement in Pt-based tri-layer structure, *Sci. Rep.* 8, 108 (2018).
 - [21] T. Chiba, G. E. W. Bauer, and S. Takhashi, Current-Induced Spin-Torque Resonance of Magnetic Insulators, *Phys. Rev. Applied* 2, 034003 (2014).
 - [22] W. L. Yang, J. W. Wei, C. H. Wan, Y. W. Xing, Z. R. Yan, X. Wang, C. Fang, C. Y. Guo, G. Q. Yu, and X. F. Han, Determining spin-torque efficiency in ferromagnetic metals via spin-torque ferromagnetic resonance, *Phys. Rev. B* 101, 064412 (2020).
 - [23] Y.-C. Lau and M. Hayashi, Spin torque efficiency of Ta, W, and Pt in metallic bilayers evaluated by harmonic Hall and spin Hall magnetoresistance measurements, *Jpn. J. Appl. Phys.* 56 0802B5 (2017).
 - [24] Y. Xu, Y. Yang, M. Zhang, Z. Luo, Y. Wu, Ultrathin All-in-One Spin Hall Magnetic Sensor with Built-In AC Excitation Enabled by Spin Current, *Adv. Mater.* 3, 1800073 (2018).
 - [25] K. Ganzhorn, J. Barker, R. Schlitz, B. A. Piot, K. Ollefs, F. Guillou, F. Wilhelm, A. Rogalev, M. Opel, M. Althammer, S. Geprägs, H. Huebl, R. Gross, G. E. W. Bauer, and S. T. B. Goennenwein, Spin Hall magnetoresistance in a canted ferrimagnet, *Phys. Rev. B* 94, 094401 (2016).
 - [26] G. R. Hoogeboom, A. Aqeel, T. Kuschel, T. T. M. Palstra, and B. J. van Wees, Negative spin Hall magnetoresistance of Pt on the bulk easy-plane antiferromagnet NiO, *Appl. Phys. Lett.* 111, 052409 (2017).
 - [27] J. Fischer, O. Gomonay, R. Schlitz, K. Ganzhorn, N.

- Vlietstra, M. Althammer, H. Huebl, M. Opel, R. Gross, S. T. B. Goennenwein, and S. Geprägs, Spin Hall magnetoresistance in antiferromagnet/heavy-metal heterostructures, *Phys. Rev. B* 97, 014417 (2018).
- [28] J. Fischer, M. Althammer, N. Vlietstra, H. Huebl, S. T.B. Goennenwein, R. Gross, S. Geprägs, and M. Opel, Large Spin Hall Magnetoresistance in Antiferromagnetic α -Fe₂O₃/Pt Heterostructures, *Phys. Rev. Applied* 13, 014019 (2020).
- [29] T. Moriyama, K. Oda, T. Ohkochi, M. Kimata, T. Ono, Spin torque control of antiferromagnetic moments in NiO, *Sci. Rep.* 8,14167 (2018).
- [30] M. Kawaguchi, D. Towa, Y.-C. Lau, S. Takahashi, and M. Hayashi, Anomalous spin Hall magnetoresistance in Pt/Co bilayers, *Appl. Phys. Lett.* 112, 202405 (2018).
- [31] Y. Du, S. Takahashi, and J. Nitta, Spin current related magnetoresistance in epitaxial Pt/Co bilayers in the presence of spin Hall effect and Rashba-Edelstein effect, *Phys. Rev. B* 103, 094419 (2021).
- [32] L. Zhou, H. Song, K. Liu, Z. Luan, P. Wang, L. Sun, S. Jiang, H. Xiang, Y. Chen, J. Du, H. Ding, K. Xia, J. Xiao, D. Wu, Observation of spin-orbit magnetoresistance in metallic thin films on magnetic insulators, *Sci. Adv.* 4, eaao3318 (2018).
- [33] Y. Yang, Z. Luo, H. Wu, Y. Xu, R.-W. Li, S. J. Pennycook, S. Zhang, Y. Wu, Anomalous Hall magnetoresistance in a ferromagnet, *Nat. Commun.* 9, 2255 (2018).
- [34] H. Hayashi, K. Ando, Orbital Hall magnetoresistance in Ni/Ti bilayers, *Appl. Phys. Lett.* 123, 172401 (2023).
- [35] S. Ding, Z. Liang, D. Go, C. Yun, M. Xue, Z. Liu, S. Becker, W. Yang, H. Du, C. Wang, Y. Yang, G. Jakob, M. Kläui, Y. Mokrousov, and J. Yang, Observation of the Orbital Rashba-Edelstein Magnetoresistance, *Phys. Rev. Lett.* 128, 067201 (2022).
- [36] S. Vélez, V. N. Golovach, A. Bedoya-Pinto, M. Isasa, E. Sagasta, M. Abadia, C. Rogero, L. E. Hueso, F. S. Bergeret, and F. Casanova, Hanle Magnetoresistance in Thin Metal Films with Strong Spin-Orbit Coupling, *Phys. Rev. Lett.* 116, 016603 (2016).
- [37] X.R. Wang, A theory for anisotropic magnetoresistance in materials with two vector order parameters, *Chin. Phys. Lett.* 39, 027301 (2022).
- [38] X.R. Wang, C. Wang, X. S. Wang, A theory of unusual anisotropic magnetoresistance in bilayer heterostructures. *Sci. Rep.* 13, 309 (2023).
- [39] L. Zhu, Q. B. Liu, and X. R. Wang, Physics origin of universal unusual magnetoresistance, *arXiv*:2410.23543
- [40] S. Langenfeld, V. Tshitoyan, Z. Fang, A. Wells, T. A. Moore, and A. J. Ferguson, Exchange magnon induced resistance asymmetry in permalloy spin-hall oscillators, *Appl. Phys. Lett.* 108, 192402 (2016).
- [41] T. Li, S. Kim, S.-J. Lee, S.-W. Lee, T. Koyama, D. Chiba, T. Moriyama, K.-J. Lee, K.-J. Kim, and T. Ono, Origin of threshold current density for asymmetric magnetoresistance in Pt=Py bilayers, *Appl. Phys. Express* 10, 073001 (2017).
- [42] Y. Yin, D.-S. Han, M. C. H. de Jong, R. Lavrijsen, R. A. Duine, H. J. M. Swagten, and B. Koopmans, Thickness dependence of unidirectional spin-hall magnetoresistance in metallic bilayers, *Appl. Phys. Lett.* 111, 232405 (2017).
- [43] T. Ideue, K. Hamamoto, S. Koshikawa, M. Ezawa, S. Shimizu, Y. Kaneko, Y. Tokura, N. Nagaosa, and Y. Iwasa, Bulk rectification effect in a polar semiconductor, *Nat. Phys.* 13, 578 (2017).
- [44] K. Olejník, V. Novák, J. Wunderlich, and T. Jungwirth, Electrical detection of magnetization reversal without auxiliary magnets, *Phys. Rev. B* 91, 180402 (2015).
- [45] K. Yasuda, A. Tsukazaki, R. Yoshimi, K. S. Takahashi, M. Kawasaki, and Y. Tokura, Large Unidirectional Magnetoresistance in a Magnetic Topological Insulator, *Phys. Rev. Lett.* 117, 127202 (2016).
- [46] K. Yasuda, A. Tsukazaki, R. Yoshimi, K. Kondou, K. S. Takahashi, Y. Otani, M. Kawasaki, and Y. Tokura, Current-Nonlinear Hall Effect and Spin-Orbit Torque Magnetization Switching in a Magnetic Topological Insulator, *Phys. Rev. Lett.* 119, 137204 (2017).
- [47] Y. Lv, J. Kally, D. Zhang, J. S. Lee, M. Jamali, N. Samarth, J.-P. Wang, Unidirectional spin-Hall and Rashba-Edelstein magnetoresistance in topological insulator/ferromagnet layer heterostructures, *Nat. Commun.* 9, 111 (2018).
- [48] I. V. Borisenko, V. E. Demidov, S. Urazhdin, A. B. Rinkevich, and S. O. Demokritov, Relation between unidirectional spin Hall magnetoresistance and spin current-driven magnon generation, *Appl. Phys. Lett.* 113, 062403 (2018).
- [49] Y. Xu, Y. Yang, Z. Luo, and Y. Wu, Disentangling magnon magnetoresistance from anisotropic and spin Hall magnetoresistance in NiFe/Pt bilayers, *Phys. Rev. B* 100 094413 (2019).
- [50] K. Hasegawa, T. Koyama, and D. Chiba, Enhanced unidirectional spin Hall magnetoresistance in a Pt=Co system with a Cu interlayer, *Phys. Rev. B* 103, L020411 (2021).
- [51] G. Liu, X.-G. Wang, Z. Z. Luan, L. F. Zhou, S. Y. Xia, B. Yang, Y. Z. Tian, G. H. Guo, J. Du, and D. Wu, Magnonic Unidirectional Spin Hall Magnetoresistance in a Heavy-Metal Ferromagnetic-Insulator Bilayer, *Phys. Rev. Lett.* 127 207206 (2021).
- [52] Y. Cheng, J. Tang, J. J. Michel, S. K. Chong, F. Yang, R. Cheng, and K. L. Wang, Unidirectional Spin Hall Magnetoresistance in Antiferromagnetic Heterostructures, *Phys. Rev. Lett.* 130 086703 (2023).
- [53] H. Sun, Y. Liu, D. Huang, Y. F., Y. Huang, M. He, X. Luo, W. Song, Y. Liu, G. Yu, and Q. L. He, Nonvolatile magnetization switching in a single-layer magnetic topological insulator, *Commun Phys* 6 222 (2023).
- [54] Y. Zhang, H. W. Zhang, and X. R. Wang, Extraordinary galvanomagnetic effects in polycrystalline magnetic films, *Europhys. Lett.* 113, 47003 (2016).
- [55] X. R. Wang, Anomalous spin hall and inverse spin Hall effects in magnetic systems, *Commun. Phys.* 4, 55 (2021).
- [56] Y. Miao, J. Sun, C. Gao, D. S. Xue, and X. R. Wang, Anisotropic Galvanomagnetic Effects in Single Cubic Crystals: A Theory and Its Verification, *Phys. Rev. Lett.* 132, 206701 (2024).
- [57] B. Han, B. Wang, Z. Yan, T. Wang, D. Yang, X. Fan, Y. Wang, and J. Cao, Determination of the Spin-Orbit Torques in Ferromagnetic-Heavy-Metal Bilayers Using Harmonic Longitudinal Voltage Measurements, *Phys. Rev. Applied* 13, 014065 (2020).
- [58] Y. Zhang, X. S. Wang, H. Y. Yuan, S. S. Kang, H. W. Zhang, and X. R. Wang, “Dynamic magnetic susceptibility and electrical detection of ferromagnetic resonance”, *J. Phys.: Condens. Matter* 29, 095806 (2017).